Proc. Natl. Acad. Sci. USA
Vol. 86, pp. 1406–1410, February 1989
Neurobiology

Low density of sodium channels supports action potential conduction in axons of neonatal rat optic nerve

(demyelinating disease/myelin/saxitoxin)

STEPHEN G. WAXMAN*†‡, JOEL A. BLACK*‡, JEFFERY D. KOCSIS*‡, AND J. MURDOCH RITCHIE†

Departments of *Neurology and †Pharmacology, Yale University School of Medicine, New Haven, CT 06510; and ‡PVA/EPVA Center for Neuroscience and Regeneration Research, Veterans Administration Medical Center, West Haven, CT 06516

Communicated by Dominick P. Purpura, November 16, 1988 (received for review October 5, 1988)

ABSTRACT **The density of sodium channels in premyelinated axons was estimated from measurements of the binding of [^{3}H]saxitoxin to neonatal rat optic nerve. The maximum saturable binding capacity of the nerve was 16.2 ± 1.2 fmol/mg of wet weight, with an equilibrium dissociation constant of 0.88 ± 0.18 nM (mean ± SEM). These values correspond to a high-affinity saxitoxin-binding site density of ≈2/μm^2 within premyelinated axon membrane. Action potential propagation in neonatal rat optic nerve is completely blocked by 5 nM saxitoxin, indicating that action potential electrogenesis is mediated by channels that correspond to high-affinity saxitoxin-binding sites. These results demonstrate that action potential conduction is supported by a low density of sodium channels in this system. Since the internodal axon membrane of myelinated fibers may contain a low density of sodium channels, it is possible that restoration of conduction in some demyelinated fibers may not require additional sodium channel incorporation into the demyelinated axon membrane.**

It is now well established that voltage-gated sodium channels mediate the inward current that underlies the action potential in most axons (1–3). Mammalian myelinated axons display a nonuniform distribution of sodium channels, which are clustered in high density in the axon membrane at the node of Ranvier but are present in very much lower density in the internodal axon membrane beneath the myelin sheath (4, 5). Inexcitability of the internodal axon contributes to the conduction failure that is seen in demyelinated fibers (4, 6). However, there is evidence that, after demyelination, continuous conduction does develop along some axons (7, 8). Indeed, morphological studies suggest that the (formerly) internodal axon membrane may reorganize after demyelination so as to develop electrical excitability (9–11).

As part of an effort to understand the mechanisms that underlie action potential conduction both in myelinated fibers and in axons that lack myelin, we have examined the development of conduction as axons develop from premyelinated axons (which lack myelin sheaths) into mature myelinated fibers. The rat optic nerve provides an especially tractable system in which to study axon membrane development of premyelinated fibers, since in the neonatal optic nerve none of the axons have yet acquired myelin sheaths, whereas in the adult virtually all the fibers are myelinated (12, 13). Previous studies have examined the morphology of the developing optic nerve (14–16) and have demonstrated action potential electrogenesis, mediated by sodium channels, in axons of the neonatal optic nerve prior to ensheathment by myelin-forming oligodendrocytes (13). However, although the sodium channel density in adult optic nerve has been estimated in saxitoxin (STX)-binding studies (17), the sodium channel density in developing optic nerve prior to myelination has not been studied. Moreover, the possibility of STX-insensitive sodium channels (which have been observed in some developing systems; ref. 18) has not been examined. In the present study, we used [^{3}H]STX, a ligand that binds in a 1:1 stoichiometry to sodium channels (19), to estimate the density of STX-sensitive sodium channels in premyelinated fibers in neonatal rat optic nerve. We also examined action potential conduction after exposure to low concentrations of STX to determine whether STX-insensitive channels contribute to action potential electrogenesis in this system.

The results presented here provide evidence for a low density (about 2/μm^2) of sodium channels with a high affinity for STX in axons of the neonatal rat optic nerve. Our results also show that action potential electrogenesis is blocked by low concentrations of STX in neonatal optic nerve and thus provide evidence that sodium channels with a high affinity for STX mediate electrogenesis in this system. Taken together, these observations indicate that low densities of sodium channels can support action potential conduction in small caliber (about 0.2-μm diameter) fibers. The predicted spacing between sodium channels (≈1 μm along the fiber axis) is surprisingly large and suggests that conduction in these fibers may occur in a "microsaltatory" manner. Moreover, the demonstration of an unexpectedly low sodium channel density, in premyelinated axons that can sustain conduction of action potentials, has important implications in terms of understanding the prerequisites for conduction in demyelinated axons.

METHODS

For morphological study, four neonatal (<2 days) Long Evans rats were anesthetized and perfused through the heart, first with a phosphate-buffered saline solution at room temperature and then with 2% paraformaldehyde and 2% glutaraldehyde in 0.14 M Sorensen's phosphate buffer (pH 7.4). After perfusion, optic nerves were carefully excised, immersed in fresh fixative, and cut into 1- to 2-mm segments. Tissue was postfixed in 2% OsO_4 in buffer for 2 hr at 4°C, dehydrated in graded ethanol solutions, and embedded in Epon.

Thin sections were cut from one block for each animal and placed on Formvar-coated slot grids, with the full cross-sectional area of the optic nerve section visible. A series of electron micrographs was obtained and printed at a final magnification of ×70,000 to give a continuous montage across the greatest diameter of the optic nerve. From each montage, 6–15 micrographs were selected at random for morphometric analysis.

Membrane surface densities (surface area of membrane per unit volume) of premyelinated axons and glial cells were measured according to standard stereologic methods (20). Measurements were carried out by using a transparent test screen, with test lines 2 cm in length and having two

The publication costs of this article were defrayed in part by page charge payment. This article must therefore be hereby marked "*advertisement*" in accordance with 18 U.S.C. §1734 solely to indicate this fact.

Abbreviations: IMP, intramembranous particle; STX, saxitoxin.

endpoints each; 50 lines were arranged in an orthogonal lattice. The test screen was placed over the electron micrograph; surface densities (S_v) of axon and glial membranes were derived from the number of intersection points (I_i) with the surface contour of the membrane profiles. The variables are related by the following equation: $S_v = 2 \times (I_i/L_t)$, where L_t = one-half of the number of endpoints of the lines overlying the optic nerve multiplied by the line length.

For STX-binding studies, two groups of optic nerves were pooled from 110 and 62 neonatal (<2 days) rats, respectively. The rats were anesthetized by exposure to 100% CO_2, decapitated, and their optic nerves were rapidly excised ≈1 mm distal (relative to the retina) to the globe and just proximal to the chiasma. The nerves were kept on ice while the dissection proceeded and then were weighed. The lengths of 16 of these optic nerves were measured prior to weighing, yielding a wet weight per millimeter of optic nerve length. Following weight determination, rat optic nerves were gently homogenized in a Duall glass homogenizer. [^{3}H]STX binding to the homogenate was then determined in triplicate at each of a variety of concentrations (19). Briefly, triplicate 200-μl samples of the homogenate (0.5 mg of wet weight nerve) were equilibrated for 20 min at several [^{3}H]STX concentrations in the absence and presence of a large concentration of unlabeled STX. After centrifugation, the uptake of [^{3}H]STX at each concentration was determined. The [^{3}H]STX solution also contained [^{14}C]mannitol as an extracellular marker, which allowed correction for the extracellular [^{3}H]STX in the pellet. Specific activity of the [^{3}H]STX was 52 dpm/fmol, and its radiochemical purity was 85%. Protein determinations were made on representative samples (21). The uptakes were then fitted to the sum of a rectangular hyperbolic component, representing specific uptake by the sodium channels, and a linear nonspecific component. Curves were fitted using a least-squares Patternsearch procedure (22).

At the end of the binding experiments, the activity of the [^{3}H]STX was assayed by binding to homogenized rabbit brain (23); this permitted comparison of binding activity for the [^{3}H]STX used in the present experiment with binding activity of toxin used in earlier studies.

Conduction properties of neonatal (0–2 day old) rat optic nerves were studied by using *in vitro* electrophysiological techniques. The optic nerves were carefully removed and placed in a submersion-type brain-slice chamber maintained at 35°C. An insulated tungsten microelectrode was positioned in the nerve for stimulation, and glass electrodes filled with 3.0 M NaCl were used to obtain field potential recordings of the compound action potential. Details of electrophysiological techniques have been described (24).

RESULTS

In optic nerves from neonatal (<2 day) rats, all axons are premyelinated (Fig. 1). The axons are termed premyelinated because, by adulthood, virtually all rat optic nerve axons will acquire myelin sheaths (13). The axons are fairly uniform in diameter (mean ± SD = 0.22 ± 0.04 μm; ref. 25) and are surrounded by abundant extracellular space. At this stage of development, there are ≈216,600 axons (26). Growth cone profiles are not present in the neonatal rat optic nerve since, by birth, most axons have reached their central targets (27). Relatively few glial cells are present at this age, and the processes from these cells are generally oriented perpendicular to the axons. In the 2-day-old optic nerve, glial ensheath-

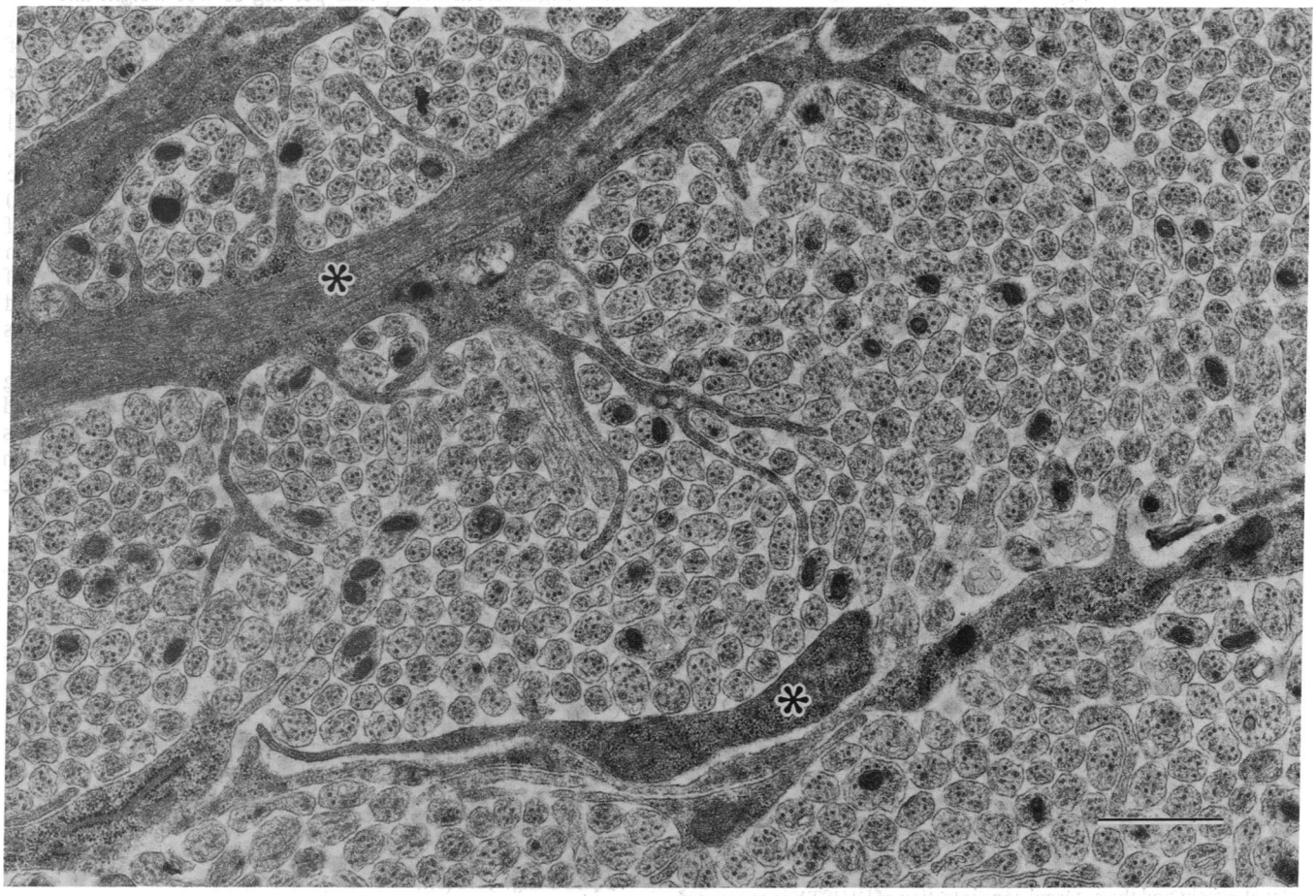

FIG. 1. Electron micrograph of a transverse section through the neonatal optic nerve. Premyelinated fibers are fairly uniform in diameter and are oriented parallel to each other. Glial processes (*) are often oriented perpendicular to the axons. (Bar = 1.0 μm).

ment of individual axons (i.e., wrapping of the entire axonal circumference by a glial process) was not observed.

Morphometric analysis of neonatal rat optic nerve yielded surface densities (mean ± SD) of axon and glial membranes of 11.5 ± 2.4 $\mu m^2/\mu m^3$ and 2.0 ± 0.8 $\mu m^2/\mu m^3$, respectively.

Fig. 2 shows the combined results obtained in two separate [^{3}H]STX-binding experiments. The points are well-fitted by a curve defined by the equation:

$$U = b[\mathrm{STX}] + \left\{M/\left(1 + \frac{K}{[\mathrm{STX}]}\right)\right\},$$

where M is the maximum saturable binding capacity, K is the equilibrium dissociation constant, [STX] is the concentration of STX, and b is a constant coefficient. STX uptake is thus the sum of a linear and a saturable (hyperbolic) component of binding. Analysis of the data indicates a saturable binding component of 16.2 ± 1.2 fmol/mg of wet weight (403 ± 29 fmol/mg of pellet protein) and an equilibrium dissociation constant of 0.88 ± 0.18 nM (mean ± SEM).

The wet weight per unit length was determined to be 0.028 mg/mm, which gives an uptake of 0.45 fmol/mm. This value, together with the calculated value of 0.15 × 10^9 μm^2 of axon membrane per mm of optic nerve (from number and size of axons in optic nerve), suggests a sodium channel density of 1.8/μm^2 for premyelinated axon membrane. This estimate is based on the assumption that sodium channels are not clustered (i.e, that they are distributed uniformly along the axons). It should be noted that this calculated sodium channel density is a maximum value, since the axolemmal area is a minimal value; it is based on the assumption that the axons are perfectly circular in cross-section.

A test on the binding of [^{3}H]STX to homogenized rabbit brain was carried out at the end of the binding experiments; this calibration gave an uptake of 136 fmol/mg of wet weight, a value that is comparable to that usually found (cf. 95 fmol/mg of wet weight; ref. 23).

A field potential recording corresponding to propagated action potential activity in neonatal rat optic nerve is shown in Fig. 3*A*. The action potential was completely blocked by application of 5 nM STX (Fig. 3*B*). A partial recovery of the response was observed following reintroduction of normal Krebs' solution (Fig. 3*C*).

DISCUSSION

The main findings of this study are (*i*) that the density of high-affinity STX-binding sites in neonatal rat optic nerve is considerably lower than that found previously for most other nonmyelinated axons (Table 1), and (*ii*) that these high-affinity STX-binding sites correspond to the sodium channels that mediate conduction in these axons.

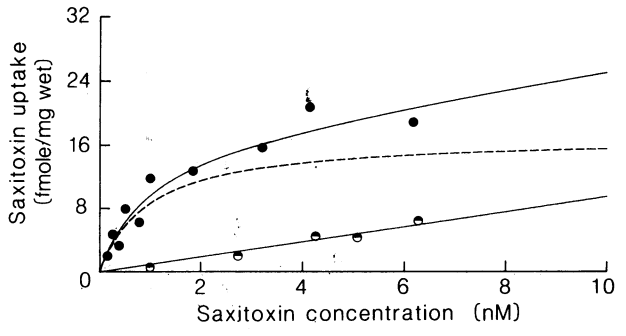

FIG. 2. The uptake of [^{3}H]STX by neonatal rat optic nerve in the absence (●) and presence (◓) of 15 μM unlabeled saxitoxin. Each point is the mean of 3–6 individual determinations. The total number of determinations was 60. The curve through the total uptake points satisfies the relation: uptake = 0.95[STX] + {16.2[STX]/([STX] + 0.88)}, where the uptake is given in units of femtomoles per milligram of wet weight and the external concentration of [^{3}H]STX is expressed in nanomoles per liter. The broken line shows the saturable component of binding.

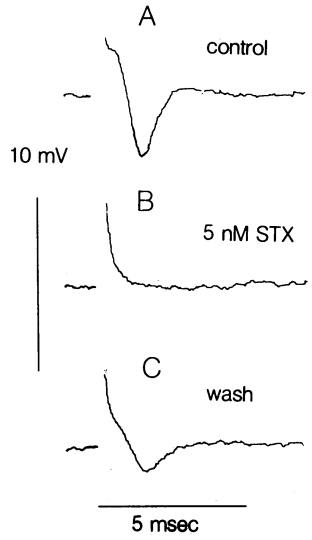

FIG. 3. (*A*) The compound action potential of a 1-day-old rat optic nerve. (*B*) Bath application of 5 nM STX resulted in complete abolition of the compound action potential. (*C*) Reapplication of normal Krebs' solution was followed by a partial recovery of the response.

The density of channels calculated above (1.8/μm^2) was based essentially on two determinations: [^{3}H]STX uptake per unit length (from the uptake per mg of wet weight and wet weight per unit length) and the number and size of axons in the optic nerve cross-section. The latter yielded a value of 0.15 × 10^9 μm^2/mm of optic nerve. An alternative estimate can be made from the morphometrically determined value of axon membrane surface density (11.5 $\mu m^2/\mu m^3$) in neonatal rat optic nerve and the total cross-sectional area of this nerve, which is 30,600 μm^2 (25). This gives a somewhat higher value of axon membrane surface area (0.35 × 10^9 μm^2/mm) presumably, in part, because it takes the noncircularity of axon cross-sections into account. This value, together with an uptake of 0.45 fmol/mm, gives a calculated density of sodium channels of 0.8/μm^2. The two values, calculated somewhat differently, thus both yield densities that are less than 2/μm^2.

The determination of the low density of [^{3}H]STX binding sites was carried out with a batch of tritiated STX that had been carefully calibrated shortly before the experiments began. Clearly, if the specific activity of the STX had fallen during the experiments, an estimate of density based on the

Table 1. Estimates of sodium channel density of unmyelinated axon membrane from [^{3}H]STX binding studies

Nerve	Sodium channel density, no. per μm^2	Mean diam., μm	Ref.
Bullfrog olfactory nerve	5	0.15	32
Necturus optic nerve	24	0.1–1.5*	28
Garfish olfactory nerve	35	0.24	19
Rabbit vagus nerve	110	0.7	19
Rat cervical sympathetic trunk	200	≈1.0	29
Squid *Loligo pealii*, giant axon	170	450	30
Squid *Loligo forbesi*, giant axon	290	450	31

*Range of axonal diameters.

original calibration would be erroneously low. However, since the [^{3}H]STX was stored at −70°C, where loss of label is virtually nonexistent (23), this possibility is unlikely. Furthermore, binding of [^{3}H]STX to rabbit brain, carried out at the end of the present experiments, yielded uptakes similar to those observed in previous studies (23). Thus, the value of about 2 binding sites per μm^2 for neonatal optic nerve is unlikely to be artifactually small.

For the calculations of the sodium channel density within premyelinated axon membrane, the binding of [^{3}H]STX to glial membranes is considered negligible. However, cultured rat astrocytes are estimated to have about 10 sodium channels per μm^2 (33). If the immature glial cells within neonatal rat optic nerve were to possess this density of sodium channels, then, given the surface density of glial membrane ($2.0\ \mu m^2/\mu m^3$), *all* the [^{3}H]STX binding within neonatal optic nerve could be accounted for by binding to glial membranes. It is unlikely that all of the STX-binding sites are on glial membranes, since conduction of action potentials is mediated by STX-sensitive sodium channels in the neonatal rat optic nerve. In any case, the presence of STX-binding sites on glia would lead to a lower, rather than higher, estimate for axon membrane sodium channel density.

Since previous studies have characterized the freeze-fracture ultrastructure of the axon membrane within rat optic nerve at various stages of development (14, 15), it is possible to compare the distribution of intramembranous particles (IMPs) with the density of [^{3}H]STX binding sites. It has been suggested that, in frog olfactory axons, some P-face particles with a 11.5- to 14.0-nm diameter correspond to STX receptors (34). However, comparison of freeze-fracture results in frog olfactory axons reveals a density of 15–18/μm^2 of IMPs for this category (32), compared to about 6/μm^2 for STX-binding sites. In neonatal optic nerve, there are ≈50 IMPs per μm^2 of 12.0- to 14.4-nm diameter in premyelinated axon membrane (14). These observations, therefore, do not support a 1:1 correlation between IMPs in any simple size class and sodium channels. This finding is not totally unexpected, since the axon membrane must contain a variety of channels, pumps, and other intramembranous proteins. For example, it has been shown that potassium channels, sensitive to 4-aminopyridine, contribute to action potential electrogenesis in neonatal rat optic nerve (13).

The finding of a low sodium channel density in neonatal rat optic nerve was especially surprising in view of previous studies (13) that demonstrated conduction of action potentials with a conduction velocity at 37°C of about 0.2 m/sec in axons of neonatal rat optic nerve. These earlier studies showed that the action potential is abolished by 1 μM tetrodotoxin and by replacement of bath sodium with the impermeant cation Tris. Moreover, there is no evidence of calcium conductance along axon shafts in the neonatal rat optic nerve (13). In the present study, we demonstrate that action potential conduction in neonatal rat optic nerve is blocked by 5 nM STX. This is close to the value predicted, on the basis of the dissociation constant demonstrated in our binding experiments (0.88 nM), to block conduction. Thus, it is unlikely that STX-insensitive sodium channels (18) contribute to action potential electrogenesis in neonatal optic nerve. We conclude that STX-sensitive sodium channels, although present in small numbers, support conduction of action potentials along these neonatal premyelinated axons.

Conduction velocity in the immature rat optic nerve increases prior to myelination; it nearly doubles between 0 and 8 days postnatal (13). During this period, the increase in axonal diameter is sufficient to account for only a 20% increase in conduction velocity. These results from optic nerve, together with data from developing peripheral nerve (35), suggest that there are changes in intrinsic membrane properties of axons during development (13). It is possible that, in premyelinated optic nerve axons at ages >2 days, sodium channel densities increase above 2/μm^2.

The sodium channel densities that we have demonstrated in neonatal rat optic nerve fibers are substantially below those predicted to maximize conduction velocities in squid giant axons (36, 37). However, even a small number of channels would be expected to depolarize the neonatal optic nerve axons to threshold because of the high input resistance (R_{in}) of these fibers. In general, for uniform cylindrical axons,

$$R_{in} = (R_m R_i/2)^{1/2}/(2\pi a^{3/2}),$$

where R_m and R_i = membrane resistance and intracellular resistivity, respectively, and a = axonal radius (38). For a 0.2-μm diameter fiber, if $R_m = 1000\ \Omega\cdot cm^2$ and $R_i = 40\ \Omega\cdot cm$, then $R_{in} \approx 7 \times 10^8\ \Omega$. Hille (39) has suggested that, in a 0.6-μm diameter fiber with an input resistance of $1.3 \times 10^8\ \Omega$, the opening of two sodium channels should depolarize the fiber to threshold. In the smaller fibers of the neonatal rat optic nerve with a nearly 5-fold greater input resistance, the opening of a very small number of sodium channels may well lead to a regenerative action potential.

On the assumption that sodium channels are randomly deployed at a density of 2/μm^2 along premyelinated axons with a mean diameter of ≈0.2 μm, the average spacing between sodium channels measured along the length of the fiber should be about 0.8 μm. Since action potentials are conducted along the neonatal rat optic nerve at 0.2 m/sec at 37°C (13), it would be expected that sodium channels would be excited at intervals of about 4 μsec. This interchannel conduction time is only 5-fold lower than the internodal conduction time for transmission of the action potential from one node of Ranvier to the next in mammalian myelinated fibers (40). The relatively low sodium channel density in these fibers suggests that channels are activated sequentially in relative spatial isolation from each other, with the action potential moving along the fibers by microsaltatory conduction.

The present results may have important implications for recovery of conduction after demyelination (4, 6). It has been demonstrated that conduction can proceed through demyelinated fibers if there is a sufficient density of sodium channels in the demyelinated axon membrane (7, 8, 41). The present findings suggest that, in some small-diameter fibers, even low densities of sodium channels can support the conduction of action potentials. In this regard, it is interesting to recall that central myelinated fibers can exhibit diameters as small as 0.2 μm (42, 43). The mean axonal diameter of myelinated fibers in adult rat optic nerve is 0.77 μm (13). Pathological studies show that the axonal diameter is often reduced in demyelinated regions (44). In addition to facilitating conduction by overcoming the impedance mismatch that occurs in demyelinated regions (45–47), this reduction in diameter may increase the input resistance of the demyelinated axon so that even a small number of sodium channels can support the conduction of action potentials. Moreover, it is possible that, following demyelination, axonal diameter is reduced without a loss of sodium channels from the demyelinated axon region. Since the available evidence suggests that some sodium channels may be present in the internodal axon membrane (4, 5, 48, 49), it is possible that relatively small (<0.5 μm) reductions in diameter may mediate restoration of conduction in some demyelinated fibers without imposing the need for additional sodium channel incorporation into the axon membrane.

We thank Ms. Bettina McKay for excellent technical assistance and Dr. Beth Friedman for critical reading of the manuscript. This work was supported in part by grants from the National Institutes of Health (NS 24931, NS 08304, and NS 12327) and the National

Multiple Sclerosis Society (RG 1231 and RG 1162) and by the Medical Research Service, Veterans Administration.

1. Huxley, A. F. & Stämpfli, R. (1951) *J. Physiol. (London)* **112,** 496–508.
2. Hodgkin, A. L. & Huxley, A. F. (1952) *J. Physiol. (London)* **117,** 500–544.
3. Dodge, F. A. & Frankenhaeuser, B. (1959) *J. Physiol. (London)* **148,** 188–200.
4. Ritchie, J. M. & Rogart, R. B. (1977) *J. Physiol. (London)* **269,** 342–354.
5. Waxman, S. G. & Quick, D. C. (1977) *J. Neurol. Neurosurg. Psychiat.* **40,** 379–386.
6. Waxman, S. G. (1977) *Arch. Neurol.* **34,** 585–590.
7. Bostock, H. & Sears, T. (1976) *Nature (London)* **263,** 786–787.
8. Bostock, H. & Sears, T. (1978) *J. Physiol. (London)* **280,** 273–301.
9. Foster, R. E., Whalen, C. C. & Waxman, S. G. (1980) *Science* **210,** 661–663.
10. Coria, F., Silos, I., Fernandez, R., Monton, F. & Lafarga, M. (1985) *Neurosci. Lett.* **58,** 359–364.
11. Black, J. A., Waxman, S. G. & Smith, M. E. (1987) *J. Neuropathol. Exp. Neurol.* **46,** 167–184.
12. Forrester, J. & Peters, A. (1967) *Nature (London)* **214,** 245–247.
13. Foster, R. E., Connors, B. W. & Waxman, S. G. (1982) *Dev. Brain Res.* **3,** 371–386.
14. Black, J. A., Foster, R. E. & Waxman, S. G. (1982) *Brain Res.* **250,** 1–20.
15. Oldfield, B. J. & Bray, G. M. (1982) *J. Neurocytol.* **11,** 627–640.
16. Hildebrand, C. & Waxman, S. G. (1984) *J. Comp. Neurol.* **224,** 25–37.
17. Pellegrino, R. G. & Ritchie, J. M. (1984) *Proc. R. Soc. London Ser. B* **222,** 155–160.
18. Frelin, C. N., Vijverberg, H. P. M., Romey, G., Vigne, P. & Lazdunski, M. (1984) *Pflügers Arch.* **402,** 121–128.
19. Ritchie, J. M., Rogart, R. B. & Strichartz, G. (1976) *J. Physiol. (London)* **261,** 477–494.
20. Weibel, E. R., Kistler, G. S. & Scherle, W. F. (1966) *J. Cell Biol.* **30,** 23–38.
21. Lowry, O. H., Rosebrough, N. J., Farr, A. L. & Randall, R. J. (1951) *J. Biol. Chem.* **193,** 265–275.
22. Colquhoun, D. (1971) *Lectures on Biostatistics* (Clarendon, Oxford).
23. Ritchie, J. M. & Rogart, R. B. (1977b) *Mol. Pharmacol.* **13,** 1136–1146.
24. Poolos, N. P., Mauk, M. D. & Kocsis, J. D. (1987) *J. Neurophysiol.* **58,** 404–416.
25. Black, J. A., Waxman, S. G., Ransom, B. R. & Feliciano, M. D. (1986) *Brain Res.* **380,** 122–135.
26. Crespo, D., O'Leary, D. D. M. & Cowan, W. M. (1985) *Dev. Brain Res.* **19,** 129–134.
27. Lund, R. D. & Bunt, A. H. (1976) *J. Comp. Neurol.* **165,** 247–264.
28. Tang, C. M., Strichartz, G. R. & Orkand, R. K. (1979) *J. Gen. Physiol.* **74,** 626–642.
29. Pellegrino, R. G., Spencer, P. S. & Ritchie, J. M. (1984) *Brain Res.* **305,** 357–360.
30. Strichartz, G. R., Rogart, R. B. & Ritchie, J. M. (1979) *J. Membr. Biol.* **48,** 357–364.
31. Keynes, R. D. & Ritchie, J. M. (1984) *Proc. R. Soc. London Ser. B* **189,** 81–86.
32. Strichartz, G. R., Small, R. K. & Pfenninger, K. H. (1984) *J. Cell Biol.* **98,** 1444–1452.
33. Ritchie, J. M. (1986) *Ann. N.Y. Acad. Sci.* **479,** 385–401.
34. Small, R. K. & Pfenninger, K. H. (1984) *J. Cell Biol.* **98,** 1422–1433.
35. Cullheim, S. & Ulfhake, B. (1979) *J. Comp. Neurol.* **188,** 679–686.
36. Hodgkin, A. L. (1975) *Philos. Trans. R. Soc. London Ser. B* **270,** 297–300.
37. Adrian, R. H. (1975) *Proc. R. Soc. London Ser. B.* **189,** 81–86.
38. Jack, J. J. B., Noble, D. & Tsien, R. W. (1975) *Electric Current Flow in Excitable Cells* (Clarendon, Oxford), pp. 31–32.
39. Hille, B. (1970) *Prog. Biophys. Mol. Biol.* **21,** 1–32.
40. Rasminsky, M. & Sears, T. A. (1972) *J. Physiol. (London)* **227,** 323–350.
41. Waxman, S. G. & Brill, M. H. (1978) *J. Neurol. Neurosurg. Psychiat.* **41,** 408–417.
42. Waxman, S. G. & Bennett, M. V. L. (1972) *Nature (London) New Biol.* **238,** 217–219.
43. Bishop, G. H. & Smith, J. M. (1964) *Exp. Neurol.* **9,** 483–501.
44. Prineas, J. W. & Connell, F. (1978) *Neurology* **28,** Part 2, 68–75.
45. Waxman, S. G. (1978) *Neurology* **28,** Part 2, 27–34.
46. Sears, T. A., Bostock, H. & Sherratt, M. (1978) *Neurology* **28,** Part 2, 21–26.
47. Waxman, S. G. & Wood, S. L. (1984) *Brain Res.* **294,** 111–122.
48. Waxman, S. G., Black, J. A. & Foster, R. E. (1983) *Int. Rev. Neurobiol.* **24,** 433–485.
49. Chiu, S. Y. & Schwarz, W. (1987) *J. Physiol. (London)* **74,** 629–642.